MATHEMATICAL BIOSCIENCES
AND ENGINEERING
Volume **8**, Number **1**, January **2011**

doi:10.3934/mbe.2011.8.21

pp. **21–48**

MULTIPLE OUTBREAKS FOR THE SAME PANDEMIC: LOCAL TRANSPORTATION AND SOCIAL DISTANCING EXPLAIN THE DIFFERENT "WAVES" OF A-H1N1PDM CASES OBSERVED IN MÉXICO DURING 2009

Marco Arieli Herrera-Valdez, Maytee Cruz-Aponte
and Carlos Castillo-Chavez

Mathematical, Computational, and Modeling Sciences Center
Physical Sciences A, P.O. Box, 871904, Tempe, AZ 85287-1904, USA

Abstract. Influenza outbreaks have been of relatively limited historical interest in México. The 2009 influenza pandemic not only changed México's health priorities but also brought to the forefront some of the strengths and weaknesses of México's epidemiological surveillance and public health system. A year later, México's data show an epidemic pattern characterized by three "waves". The reasons this three-wave patterns are theoretically investigated via models that incorporate México's general trends of land transportation, public health measures, and the regular opening and closing of schools during 2009. The role of vaccination is also studied taking into account delays in access and limitations in the total and daily numbers of vaccines available. The research in this article supports the view that the thee epidemic "waves" are the result of the synergistic interactions of three factors: regional movement patterns of Mexicans, the impact and effectiveness of dramatic social distancing measures imposed during the first outbreak, and the summer release of school children followed by their subsequent return to classes in the fall. The three "waves" cannot be explained by the transportation patterns alone but only through the combination of transport patterns and changes in contact rates due to the use of explicit or scheduled social distancing measures. The research identifies possible vaccination schemes that account for the school calendar and whose effectiveness are enhanced by social distancing measures. The limited impact of the late arrival of the vaccine is also analyzed.

1. **Introduction.** We live in a highly interconnected world where individuals move between cities, states, countries, and continents in a matter of hours. Several studies have looked at the role of movement of individuals or transportation patterns on the recurrence of influenza epidemic outbreaks [40]. The first efforts to connect epidemic patterns explicitly to train-transportation flows where conducted by [9, 63], and most recently by [40], and [43]. The transmission and evolution of the influenza virus is influenced by local and global individual patterns of movement, massive demographic growth, and the diversity and availability of domestic and wild animal populations, a key reservoir of genetic variability [65, 14]. Unfortunately, despite the severity of single epidemic outbreaks and the availability of the earlier work of Kermack and McKendrick [42] most of the theoretical work on influenza has

2000 *Mathematics Subject Classification.* Primary: 58F15, 58F17; Secondary: 53C35.

Key words and phrases. Influenza, local transportation, social distancing, multiwave epidemics.

MAHV and MCA were supported by the Mathematical, Computational, and Modeling Sciences Center, Arizona State University.

been driven by concerns over its long-term dynamics and/or A-subtype specific coevolutionary dynamics [16, 17, 5, 62]. Further, the role of behavior in epidemic outbreaks has been explored in rather limiting settings [36, 12, 29, 34]. The impact of "social-distancing" and information on disease dynamics have gained relevance and importance during the last few years; a reinvigorated research direction by the impact of this 2009 A/H1N1 influenza pandemic [58, 69, 4, 10, 56]. Fortunately, theoretical extensions of the single outbreak models [42] have been carried out by various researchers, most notably F. Brauer [11]. In fact, a detailed account on recent advances in modeling influenza outbreaks can be found in this volume [13].

FIGURE 1. **Initial influenza outbreak and the historical influenza corridor.** A/H1N1 epidemic outbreak in México by region 2009. The Mexican States that contributed with more than half of the total cases during the initial spread of A/H1N1 up to June 4, 2009 are shown in dark gray (see Fig. 3). The remaining States (light gray) were the main contributors to secondary outbreaks later in the year. The red dots mark states in the historical influenza corridor (Acuña-Soto, personal communication, see also [2] and Figs. 2).

The study of the dynamics of influenza outbreaks in México must account for México's unique characteristics. México is a highly centralized country in which the massive transportation of individuals occurs predominantly by land with México City as the main hub for most traffic (air transportation inclusive). México City has four "Central Bus Terminals", connected by a subway system that moves 5 million people per day. In addition, there are 80 thousand taxicabs generating about 780 thousand rides daily [51] and a public city bus system with 11 main lines that moves approximately eight million users per day [32]. Influenza does not seem to follow uniform transmission patterns along México. In fact, it seems to "primarily" travel through what [1] has coined as Mexico's *influenza corridor* (Fig. 1, red dots). This corridor extends from south to north along central México and is bounded by two mountain ranges, the West and East Sierra Madres. This geographical distinction seems to be supported by recent preliminary analysis of historical data of upper respiratory illnesses in México. The origins of "the" corridor are not entirely clear

but the abundance of some metals and other minerals, and the historical patterns of commercial activity may constitute some of the underlying factors [44]. In fact, there is a large overlap between the States in "the" corridor (Fig. 1 red dots) and the States that collectively reported more than half of the cases of pandemic influenza A-H1N1 (A-H1N1pdm) during the first wave up to June 4, 2009 (about 12 weeks, Fig. 1 dark gray).

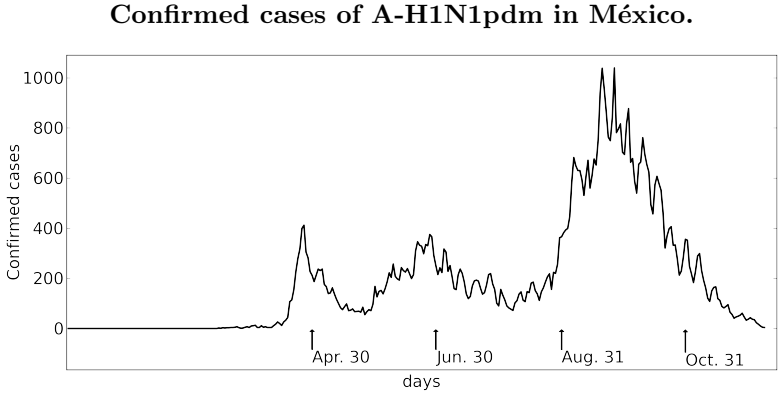

FIGURE 2. **A-H1N1pdm epidemic outbreak in México during 2009.** Daily confirmed cases by RT-PCR reported by Mexican authorities [66]. January 1, 2009 is considered as day 1 and the last day was approximately December 25, 2009. From [66]. Social distancing and school closures were imposed in April 29, 2009. The official summer school closure occurs at the end of June and mid December, and fall classes start around Sept. 1.

The A-H1N1 pandemic of 2009 in México was characterized by three "waves" of morbidity and mortality (Fig. 2). For comparison, past pandemics have been characterized by the occurrence of multiple "waves" over short time periods [52, 22]. However, the size of the individual contributions from different geographical regions within México to these "waves" is not uniform (Fig. 3A,B). These "waves" took shape during the year as data aggregated over time. What are the drivers of these epidemic "waves"? One possibility is that non-uniform aggregation of the data is due to delays in transmission that, in turn, were caused social distancing measures, movement of people, and population density. Can these "waves" be explicitly tied in to transportation patterns, behavioral changes, and the regular school calendar schedule in México?

We investigate the influence of México City as a hub on the spatio-temporal patterns of spread of A-H1N1pdm cases during 2009 (Fig. 2) by assuming that the different Mexican States and the Federal District (DF) form a star-shaped graph with vertices representing the flow to, or from DF. To do so, we combine official case data from the Mexican health authorities (Figs. 2 and 3A,B) and empirically estimated flows from observations collected at toll gates located at the different entry points to DF, taking into consideration a set of dates from 2009 hypothesized as important for the introduction of delays in the propagation of A-H1N1pdm in México. We identify scenarios that result in multiple epidemic "waves" due to the synergistic interactions between transportation flow patterns and changes in the

contact rates between individuals. It is observed that both of these factors induce delays in the evolution of influenza dynamics that cause the data to aggregate nonuniformly across different regions in México, displaying patterns consistent with the existing data shown in Figs. 2 and 3.

The rest of this article is organized as follows: A qualitative analysis of the main events related to the A-H1N1pdm epidemic in México is made first, followed by a description of the model. Simulations where the influence of transport flow, social distancing, and school closures on the time course of the epidemic are presented first, followed by simulations of the effects of vaccination with different arrival times during the year. We finish this article with a discussion and final remarks.

2. Qualitative analysis of the A-H1N1pdm epidemic in México during 2009.

Three different reports of the number of A-H1N1pdm cases confirmed by real time polymerase chain reaction (RT-PCR) in México, ordered by the States, are shown in Fig. 3A. The difference between the three reports is collected in Fig. 3B. The data in these figures (Fig. 3A-B) support the view that the first outbreak affected mostly States shown on the left portion of panel A (e.g. Distrito Federal, San Luis Potosí, etc. indicated by the line corresponding to June 4, 2009); the States in the right portion of the graph (e.g. Sinaloa, Coahuila, etc in later reports), reported significant numbers of confirmed cases during the summer; while States like Baja California or Sonora did not experienced an outbreak until the fall. The majority of the States that contributed the most A-H1N1pdm cases during the initial phase of the outbreak have been identified as members of México's influenza corridor (Fig. 1).

The first official case of novel swine-origin influenza disease was identified in Oaxaca [47, 24]. The diseased was a diabetic woman originally identified as a probable SARS case around March 5, 2009; she died of atypical pneumonia a few days later. A small outbreak of influenza-like illness was also reported in the town of La Gloria, Veracruz, between March 10 and April 6, 2009. About one fourth of the local population was affected but there were no hospitalizations [50, 66]. The first confirmation that a novel strain of type A influenza was circulating in México and affecting primarily a young population [20] was made in April 23, 2009 by the National Microbiology Laboratory in Canada. The report was based on two apparently unrelated cases, the woman from Oaxaca and a five year old child from La Gloria. An epidemiological alert was issued by The National Committee on Epidemiological Surveillance in México on April 16. On April 17, the United States Center for Disease Control started reporting cases of a new A-H1N1pdm strain. On April 18, the media spread the outbreak news while an ongoing alert on severe pneumonia cases had just been set in México City. On April 22, a large number of severe pneumonia cases were reported in México City, San Luis Potosí, and Oaxaca.

In response to the epidemiological alert, the government of México City implemented a series of *social distancing measures* that included school closures, closure of public spaces, and the cancellation of public events. The rest of the Mexican States implemented the same policy within days. School closures started on April 27 while non-essential economic activities were suspended on April 30. Schools reopened after May 10 and the population slowly resumed their normal activities as the summer arrived. By the time that social distancing measures were relaxed, the behavior of people was notably modified. For instance, many individuals in México

A. Confirmed cases of A-H1N1pdm by State.

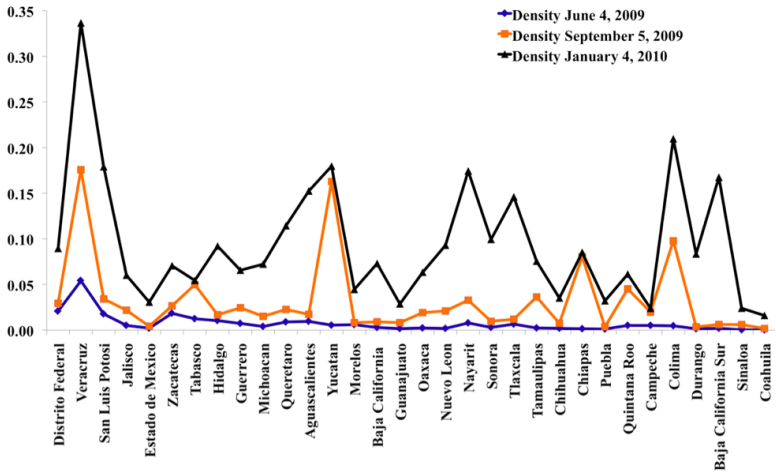

B. Difference between reports.

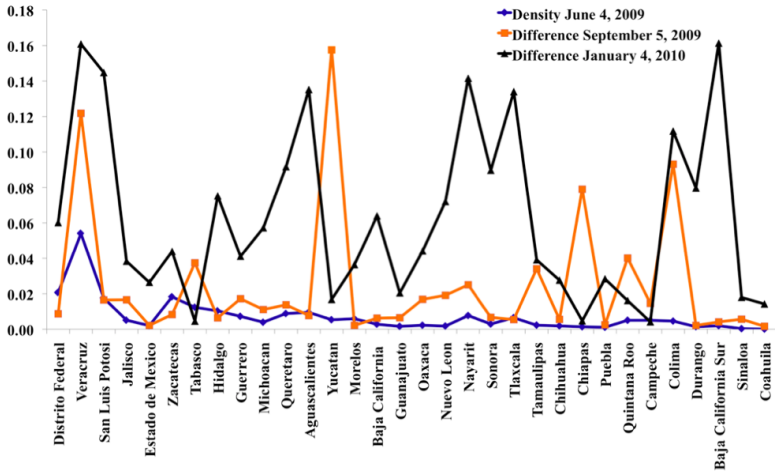

FIGURE 3. **A-H1N1pdm epidemic outbreak in México by region 2009. A.** Confirmed cases of A-H1N1pdm by State. Three different reports of confirmed cases dated June 4 and September 5, 2009, and January 4, 2010. Collection of States contributed differently to the reported total number of cases (aggregated three wave data) during the 2009-2010 pandemic. **B.** Difference between the reports shown in **A**.

were still wearing masks in public a year after the first A-H1N1pdm outbreak of 2009 was declared and hand sanitizers became part of the common office supplies.

Classes for kinder garden, elementary, middle, and high school typically end at around June 30 or earlier, marking the official start of the summer in México. Children resume school activities at the beginning of September and do not have another long break until mid December. These times during the year are regarded in this work as important landmarks for the time course of the epidemic and are modeled explicitly. The specific assumption made here is that infection rates decreased in México as a result of enforced social distancing measures, and as a consequence of the impact of school closures on contact rates [53, 70]. For instance, there were three surges in the reported cases of A-H1N1pdm in México during 2009, with peaks dated around April 30, July 1, and September 25 respectively (Fig. 2). The first peak is in line with the implementation of social distancing measures and school closures by the Mexican authorities; the second occurred soon after schools for pre-college education closed for the summer; while the third took place during the fall of 2009. The rising phase of the third wave began about the time when schools returned to classes in the fall.

2.1. **Vaccination during the pandemic.** The General Director of the World Health Organization communicated her decision to raise the A-H1N1pdm pandemic alert from phase 4 to phase 5 on April 29, 2009 [19]. It became clear soon after her announcement that the potential supply of vaccines was, at best, to be no more than 900 million [28]; that is, perhaps enough to cover 10-15% of the current world population [74]. The proportional distribution of vaccines would mean that each country would have vaccinations for about 10%-15% of its population. The number of vaccines that each country secured was in fact determined by the abundance or lack of financial resources. Massive vaccination against the novel A-H1N1pdm virus started in Canada, U.S., Northern Europe and other wealthy nations around the end of September of 2009; additional countries began to administer their share over the last months of the year. The first 650 thousand vaccines from an estimated 30 million vaccines, arrived in México on November 23, 2009 [48]. However, by the beginning of January 2010, the Secretariat of Health in México had approximately 13 million vaccines in hand, of which only 1.5 million had been administered to the general population [69]. Similar scenarios were repeated in other developing countries.

2.2. **Modeling.** Models are used to theoretically investigate the role of transportation flow and the impact of public health interventions (modulations of the infection rate of influenza) on the time course of an epidemic outbreak. This article explores the role of social distancing, school closures, transportation patterns, and vaccination policies on the time course of México's epidemic. An extension of the [42] model is constructed following the general framework originally proposed by [63]. Our modeling framework resembles the modeling approach of [7], [40], and [71].

México is divided into thirty-one States and DF; México City is contained in DF. These thirty-two regions are regarded as nodes in a star-shaped, weighted graph with all nodes connected to DF, but not directly connected to each other. In the rest of this article the Mexican States will also be referred to as *regions* to facilitate the description. The regions are indexed 0,1,...,31, with DF (México City) index by the number 0. Regions are regarded as *strongly* and *weakly connected* to D.F. (México City) according to the data from Fig. 3A,B. More specifically, regions were ordered by their contribution to the initial total cases reported by June 4, 2009. Those regions with contributions larger than the median contribution up to

June 4, 2009 are assumed to be *strongly connected* to DF. The rest of the Mexican States form the *weakly connected* group.

The infection rate is assumed to change as a function of *social distancing* measures, behavioral changes induced by the epidemiological alert, and school closures. The rates of infection and recovery periods are assumed depend on the region [7] while the interactions between individuals within a given region are assumed to be homogeneous. Populations in the so called *influenza corridor* are assumed to be more susceptible to the disease (possible driven by higher contact rates); they are also assumed to recover 2 days later than in the rest of the México [44]. The results of our analysis are not sensitive to these last assumptions. That is, small variations on the values of these parameters do not change the general results presented here.

Infected individuals are assumed to go through an *incubation period* of 2 days before becoming infectious. Once infected, the *recovery time* was assumed to be between 5 and 9 days. Disease deaths are also included in the model. Infectious individuals are further divided into confirmed and unconfirmed cases. The unconfirmed cases include individuals who had symptoms of influenza but did not seek medical care, and also those who had an asymptomatic infection [4]. It is assumed that the traveling plans of an infectious individual were not affected by symptoms. Individuals are assumed to infect others during this incubation period, at a lower rate than the infectious individuals. Also, recovered individuals gain permanent immunity against the novel A-H1N1pdm influenza virus [64, 6]. It is also assumed that there is a *limited vaccine stockpile* (see [8]; see Morales et al. in this volume). People belonging to the susceptible, incubating, infected but unconfirmed, and recovered groups are eligible for vaccination. Daily vaccination rates are not assumed to be proportional to the populations receiving vaccinations. Instead it is assumed that only a maximum number of vaccines can be administered each day (constraints of the infrastructure) thus allowing a possible saturation in the demand for vaccines.

During the spring, summer, and winter breaks, the contribution to the total flow of people in and out of México City is assumed to be nearly the same for the strongly and weakly connected States. The strongly connected populations contribute more to the total flow of people in and out of México City the rest of the year. Note, for instance, that during the initial outbreak DF is followed by the strongly, and then the weakly connected regions, as ordered by their relative contribution to the first wave of the epidemic (report of June 4, Fig. 3). It is assumed that the net daily flow of people through DF is zero, with about half a million people coming into or out of México City every day.

The contribution of each region to the daily flow through DF is determined as follows: let F, q, and N_i denote, respectively, the number of people that go through DF every day, the relative contribution of the strongly connected group to the total daily flow through DF, and the population size of the i^{th} region. The daily contribution of the i^{th} strongly connected region and the k^{th} weakly connected region are written, respectively, as

$$q_i(t) = F \cdot \frac{q(t) \cdot N_i}{\sum \{N_j : j \in J_s\}}, \quad q_k(t) = F \cdot \frac{(1 - q(t)) \cdot N_k}{\sum \{N_j : j \in J_w\}}. \tag{1}$$

where J_s and J_w are index sets for the strongly and weakly connected regions, respectively. During the school breaks $q = 1/2$, and $q >> (1 - q)$ during the rest of the year.

The flux between States given by transportation can be written with the aid of a time-dependent symmetrical matrix, $Q(t) = (Q_{ij})$ with entries defined as

$$Q_{ij} = \begin{cases} q_j(t)/N_i & \text{if } i = 0 \\ 0 & \text{otherwise} \end{cases}$$

for $0 < i, j \leq M = 31$. Here, $Q_{ij}(t)$ represents the proportion of the population from region i that travels to region j per day.

The population of each region is divided into disjoint subgroups based on the individuals epidemiological states: S, I, C, U, R, and V represent, *susceptibles, incubating, infected and confirmed, infected but not confirmed, recovered*, and *vaccinated*, respectively. A schematic of the relationships between the classes are as shown in Fig. 4.

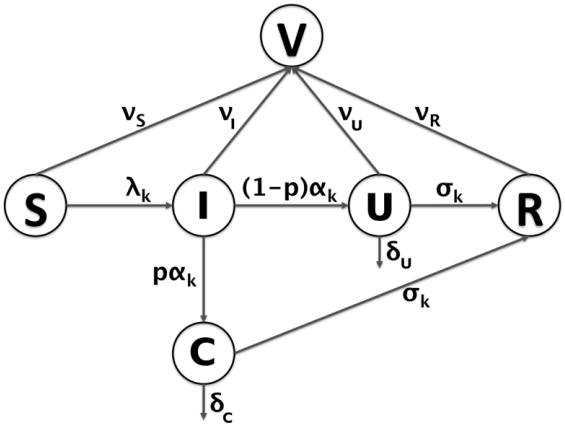

FIGURE 4. **Schematic of the flow between compartments in each of the Mexican States.**

Each of the classes S, I, C, U, R, and V is indexed by region. The infection rate for region k, β_k, represents the mean infection probability per contact where $\lambda_k(t)$ being

$$\lambda_k(t) = g(t)\frac{\beta_k}{N_k}\left(C_k + U_k + \mu_I I_k\right) \tag{2}$$

where the parameter μ_I takes values between 0 and 1 modeling a decrease in the infectivity of individuals who are within the incubation period. The contact rate is *modulated* by a function $g(t)$ to capture *social distancing and school closures* at specific dates during the year. The modulation of the infection rate was defined using a combination of sigmoid functions of the form

$$g(t) \quad = \quad \sum \{S(t; t_i, m) : i\}, \tag{3}$$

where

$$S(t; t_i, m) \quad = \quad A + \frac{B - A}{1 + \exp\left[m(t - t_i)\right]}, \tag{4}$$

with $0 < A < B < 1$. The time point at which the sigmoid reaches a value of $0.5(B-A)$ is t_i. The selected times t_i are used as anchor points for the sigmoids, at or slightly after dates when social distancing or school closures occur. The rate at which the sigmoid function changes is controlled by m, that is S is decreasing when

$m > 0$ and increasing when $m < 0$. For instance, a sharp downward sigmoid with $m = 10$ is used to represent a sudden drop in the contact rate as it happens when schools close or open, or if social distancing policies are imposed by the government. In contrast, an slowly increasing sigmoid with $m = 0.5$ is used to represent a slow recovery in the contact rate after social distancing was imposed.

TABLE 1. Parameters.

Parameter	**Description**	**Value/Range**	**Reference**
α^{-1}	incubation period	2 days	[55]
σ_k^{-1}	recovery period for State k	7 days	[25],[60]
μ_I	reduction factor for infectivity during incubation	0.5	Estimated, [59]
β_k	mean infection probability per contact for State k	0.95	Estimated, [60]
δ_x	influenza-induced death rate for $x = \{C, U\}$	10^{-6}	Estimated, [60]
p	probability of confirmed case	$[0.1, 0.3]$	Estimated
$\hat{\nu}$	maximum vaccines per day	$[1, 60] \times 10^3$/day	Estimated from Media [48, 28]
F	Thousands of people traveling to/from D.F. per day	$[500, 1000] \times 10^3$/day	México City government [27]

The *start of the epidemic* outbreak is modeled by inserting a pulse of the form

$$\varepsilon_k(t) = 0.001 \exp\left[\frac{(t - t_0)^2}{2}\right] \tag{5}$$

added to the class E_k to start the outbreak in the region k; the pulse is also subtracted from S_k. In the simulations below, ε_i is zero for all $i \neq k$; and the initially seeded regions are Oaxaca (in the south Pacific) and Veracruz (in the Golf of México). These two regions are important ports of entry of tourists and goods from the Atlantic and Pacific, respectively, and were also the two regions where the first official cases of A-H1N1pdm were reported. The peak amplitude can be thought of as one individual (0.001 in thousands). The time t_0 can thus be thought of as the start of the epidemic with (approximately) one individual in the incubating group.

The *vaccines* are assumed to be distributed on a daily basis with the system being able to deliver a maximum number of vaccines per day. The stockpiles are distributed as proportions of a total stockpile depending on policy. The number of vaccines in the initial stock pile, ν is adjusted to calculate the initial stockpile for each State

$$\nu_k = \nu \cdot w_i, \text{ for } i = 0, ..., 31. \tag{6}$$

The weights w_i are determined by setting a "vaccination policy". The vaccines in this article are proportionally distributed according to the relative population size in each region. That is, $w_i = N_i/\sum\{N_k : k = 0, ..., 31\}$. The number of vaccines used per day, per class, within the kth population, are denoted by ν_{S_k}, ν_{I_k}, ν_{U_k}, ν_{R_k} and calculated as follows: Given a maximum number of vaccines per day $\hat{\nu}$, the number of vaccines that can be used each day in the population k is $\hat{\nu}_k = \nu \cdot N_k/\sum\{N_i : i = 0, ...31\}$. Therefore, the number of vaccines that can be used in each class within a single region k is a proportion of $\hat{\nu}_k$ determined by the number of individuals in that city, and the percentage of individuals in each class of that city. For instance, for the class X in city k, the maximum number of vaccines available, ν_{X_k}, is less than or equal to $\hat{\nu}_k \cdot X_k/\sum\{X_i : i = 0, ..., 31\}$, for $X \in \{S, I, U, R\}$. The available number of vaccines for each region was calculated by subtracting $\sum\{\hat{\nu}_k : k = 0, ..., 31\}$ from the number of remaining vaccines for the region at each point in time considered in a simulation. At each point in time, the numerical implementation includes conditions that guarantee that the number of vaccinated people in a compartment does not exceed the number of people in the compartment. That is, at each point in time, $\nu_{X_k} < N_{X_k}$, for $X \in \{S, I, U, R\}$.

Equations. Having defined rates, transportation, and vaccination as above (Eqs. (1)-(6)), the system of equations describing the time-dependent change in region k is:

$$\dot{S}_k = (Q_k - \lambda_k) S_k + \sum_{i \neq k} Q_{i1} S_i - \varepsilon(t) - \nu_{S_k} \tag{7}$$

$$\dot{I}_k = (Q_k - \alpha) I_k + \sum_{i \neq k} Q_{i1} I_i + \lambda_k S_k + \varepsilon(t) - \nu_{I_k} \tag{8}$$

$$\dot{C}_k = (Q_k - \sigma_k - \delta_C) C_k + \sum_{i \neq k} Q_{i1} C_i + \alpha p I_k \tag{9}$$

$$\dot{U}_k = (Q_k - \sigma_k - \delta_U) U_k + \sum_{i \neq k} Q_{i1} U_i + \alpha(1-p) I_k - \nu_{U_k} \tag{10}$$

$$\dot{R}_k = Q_k R_k + \sum_{i \neq k} Q_{i1} R_i + \sigma_k C_k + \sigma_k U_k - \nu_{R_k} \tag{11}$$

$$\dot{V}_k = Q_k V_k + \sum_{i \neq k} Q_{i1} V_i + \nu_{S_k} + \nu_{I_k} + \nu_{U_k} + \nu_{R_k}, \tag{12}$$

$$\dot{w}_k = -(\nu_{S_k} + \nu_{I_k} + \nu_{U_k} + \nu_{R_k}) \tag{13}$$

$$\dot{D}_k = \delta_C C_k + \delta_U U_k \tag{14}$$

with variables w and D representing, respectively, the available vaccine stockpile and disease-induced deaths. All population numbers are in thousands of individuals; the time is in days with t_0 equal to January 1st, 2009. The term $Q_k = Q_{k0} - \sum\{Q_{0i} : i = 1, ..., M, i \neq k\}$ denotes the proportion of people traveling from region k to DF minus the proportion of people returning to region k.

2.3. **Data acquisition and numerical simulations.** All data presented here was obtained from the weekly reports of the Mexican Health Secretariat [66], recorded in spreadsheets using Open Office 2.3, and processed using Python 2.5 in Mac Pro notebooks running on OS X or in a Lenovo T400 laptop running Python2.6 under Ubuntu 9.10 with an Intel(R) Core(TM)2 Duo CPU T9600 at 2.8 GHz. All simulations were performed using the python module scipy [41]. Figures were

produced with the python module matplotlib [37]. Code used for simulations is available upon request.

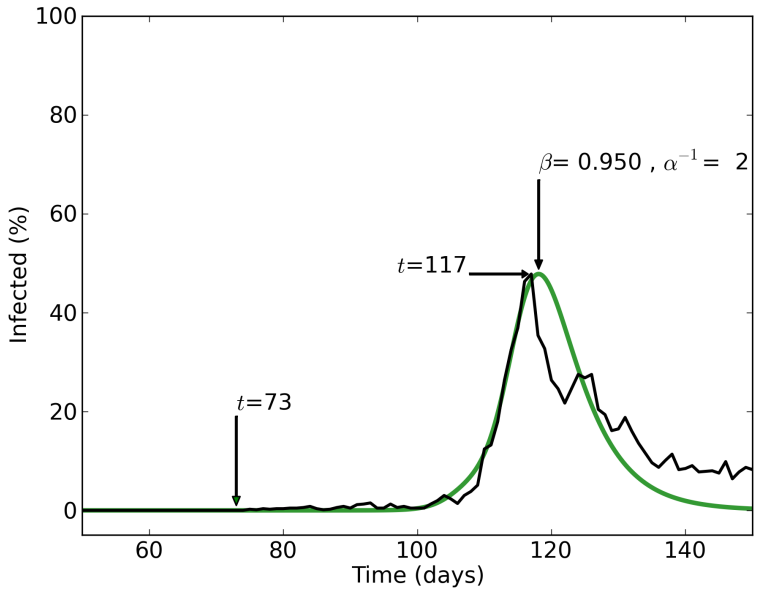

FIGURE 5. **Start of the pandemic.** Data fit for the beginning of the first wave of the pandemic. The original data (confirmed cases) and the modeled curves were normalized so that the peak was located at 1, and the infection rate and incubation recovery periods (β and $r_{infect} = \alpha$, respectively) were adjusted to fit the initial outbreak before the first peak. The resulting parameters are such that $\beta/\alpha \approx 1.9$. Day 73 corresponds to March 14. Day 117 corresponds to April 29.

3. Results.

3.1. Parameter estimation and start of the fist outbreak.

A reduced version of model (1)-(14) assuming no vaccination ($\nu = 0$) and no deaths was used to estimate parameters that best fit the curve of confirmed cases before April 29, 2009. For this initial parameter estimation, it was assumed that there were no unconfirmed cases ($p = 0$), and that the infection rate and total infectious period (incubation + infection recovery periods) of the system (2)-(14) were assumed to be the same for all States, thus yielding the "aggregated" dynamics that would be generated by a single population model [7]. To do so, the simulated total of infective (incubating, confirmed, and unconfirmed, respectively, I, C and U, for all regions) and the data for the first wave were normalized by their peaks so that both had a maximum of 1. It is worth remark at this point that the data examined does not let us test whether or not some populations in México were more susceptible to the novel A-H1N1pdm virus. However, the historical evidence on the patterns of respiratory disease support this assumption [1]. Systematic variation of the incubation period

and infectivity was performed to fit the slope of initial outbreak to the data up to the first of the three major epidemic peaks (Fig. 2 and also Fig. 5). The starting point of the epidemic was then shifted to find the time at which the initial increasing phase of the outbreak in the simulations overlapped with the initial phase of the normalized data. The death rate was carefully chosen to match the order of magnitude reported in official data ($\sim$ 100's of people, not shown). From this initial estimation, our simulations suggest that the start of the epidemic occurred approximately between days 73 and 75, which correspond to March 15-17, 2009.

After fitting the model to the first outbreak, regional variations in the parameters were introduced by adding uniformly distributed random numbers between -0.1 and 0.1 to β_k and σ_k for each $k \in \{0, ..., 31\}$. The system (1)-(14) was used to investigate the effects of transportation (weak/strong connections to DF), social distancing, and school closures on the development of the epidemic. As with the initial parameter estimation, it was assumed that there was no vaccination (ν=0, Sec. 3.2).

Simulations that include regional variations in the parameters (not shown) yield starting dates for the epidemic that are consistent with the initial estimations obtained assuming homogeneity in the parameters. In particular, simulations in which the recovery period σ_k was 1 day longer in the influenza corridor and 1 day shorter out of the corridor (not shown) yield qualitatively similar average values for the mean infection probability per contact, β_k. The overall results presented in this article are not significantly affected by the parameter variations mentioned above.

3.2. **Influence of transport, social distancing and school closure on the time course of the epidemic.**

3.2.1. *Transportation as a delay mechanism to generate multiple outbreaks.* The spread of A-H1N1pdm cases was not uniform across México. That is, not all States were hit by the epidemic at the same time, or with the same force (Fig. 3A-B, June 4 and September 4 reports, black and orange curves).

To test if land transport could be responsible for the delay observed in the epidemic outbreaks reported in the different Mexican States, simulations with the system (1)-(14) were conducted assuming different contributions of the strongly and weakly connected States (q and $1-q$, respectively) to the total daily flow from and to México City (Fig. 6). To do so, the number of confirmed cases was analyzed by region and the local spread of A-H1N1pdm during the first outbreak (Fig. 3, June 4 report) was considered explicitly in the derivation of the transportation matrix of the model (Eq. (2)). Figure 6 shows the total of infected people at each point in time (the sum of incubating (I), confirmed (C), and unconfirmed (U)) from the strongly and weakly connected States, respectively, in solid and dashed black lines. The total of infected people in the whole country is illustrated by a solid, thicker gray line. For all simulations presented here, it was assumed that the epidemic started in Veracruz and Oaxaca; note the general aspects of the results presented in this section can be obtained assuming other starting states.

A case in which all Mexican States contribute to the flow into and out of DF nearly proportionally to their population size ($q = 0.5$) is shown in Fig. 6A. The small delay between the strongly and weakly connected is mainly due to the small difference between the contributions of strongly and weakly connected States and to a less extent, from the modest levels of heterogeneity coming from infection rates and recovery periods (assumed for the different populations). If the traffic weight q for the Mexican States in the strongly connected subset is increased (i.e.

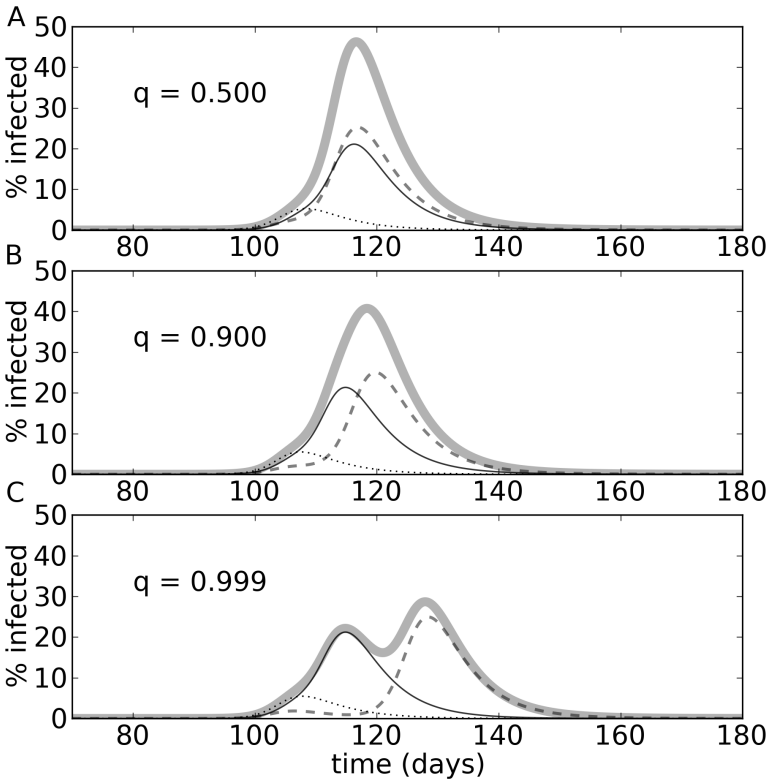

FIGURE 6. **Influence of transportation on the time course of the epidemic.** The curves represent the total of infected people including the incubating (I), confirmed (C), and unconfirmed (U) groups. The solid and dashed curves are, respectively, the infected people in strongly and weakly connected populations to D.F. The dotted line is the epidemic curve in Veracruz and Oaxaca. The thicker gray line is the total of infected people. **A.** Simulation in which strongly and weakly connected populations contribute nearly the same (q=0.5) to the total traffic through México City. **B** and **C**. Simulations in which, respectively, 9 of every 10 (q=0.9, **B**), and 999 of every 1000 (q=0.999, **C**)) individuals traveling to and from D.F. come from a strongly connected region. Other parameters: p=0.1, F=500.

it is assumed that strongly connected populations contribute more than they would according to their proportion in the total population), the delays between the peaks become larger. Fig. 6B shows the case in which 9 out of 10 individuals come from the strongly connected States. Fig. 6C shows simulations in which 999 out of every 1000 individuals traveling through México City come from the strongly connected states. In general, the delay is an increasing function of q. However, for the delay in the weakly connected regions to be similar to the delay of the secondary "wave"

observed in the epidemic, the contribution of the weakly connected states to the total traffic has to be negligible (q >0.9999, not shown). Since the case in which only one in every 100 individuals traveling in and out of DF comes from one of the weakly connected states ($q = 0.99$) is unrealistic but the delays in the total curve appear for $q > 0.99$. Therefore, we conclude that transportation may contribute to create a delay between peaks of confirmed cases for different states, but the connectivity between DF and the 31 Mexican States alone does not fully explain the different peaks delayed by several weeks shown in the data curve of total cases.

3.2.2. *Social distancing and school closures.* The first two local maximae in the epidemic curves shown in Fig. 2 occurred at times in which it is fair to assume that the contact rates suddenly decreased. In the first case, the peak is reached at, or soon after the Mexican government imposed social distancing measures and school closures. In the second case the peak is reached around June 30, which marks the end of the school year. Similarly, the first two local minima occur at times in which contact rates among the population increase after a period of reduction. The first local minimum occurs at the end of May after the social distancing measures imposed by the Mexican government were relaxed and the population resumed normal activity; social distancing measures lasted for approximately 2 weeks, after which the population slowly resumed their normal activities. The second local minimum occurs near the end of August when the school year begins.

Remarkably, many of the States located within the historical influenza corridor that were hit by A-H1N1pdm during the first "wave", continued to be affected during the summer, but some seemed to be less affected than the weakly connected states during the summer; a trend that continued in some but not all States throughout the fall (see Fig. 3A,B). The epidemic, viewed from a whole-country perspective seemed to become milder during the summer and resumed to have a much larger peak and width at the end of the summer, which marks the end of the school break.

To test the possibility that social distancing and school closure had an impact on the epidemic, and more specifically, whether these two factors contributed to the generation of the second and third outbreaks, it is assumed that the changes in contact described in previous paragraphs are captured via the time-dependent modulation of the infection rates in each state, λ_k, $k = 0, ..., 31$. To introduce a time-dependent modulation in agreement with the dates at which government policies were implemented and with the school calendar, we combined sigmoid functions (Eq. (4)) to decrease and increase the rate of infection λ_k, at specific points in time (see also Fig. 7A). The measures implemented by the Mexican government during the last days of April 2009 (before day 120) were captured by modulating the contact rate with a decreasing sigmoid with very steep amplitude. The end of the social distancing policy and subsequent return to normal activity was represented by an increasing sigmoid with a slower slope compared to that of the implementation of government policies. The final value of this second, increasing sigmoid function was such that the infection rate could be lower than the initial infection rate. The lower value is justified by the fact that behavioral changes occurred during the days and months following the start of the epidemic. Similar constructions were used to model the end of classes at the end of June (around day 180) and the reopening of schools in September (before day 240). The resulting modulating function for the infection rate, $g(t)$, was varied by changing the slopes and final values for each of the sigmoid functions. The last value of this modulation function reflects long-term behavioral changes that occurred during the beginning of the epidemic Fig. 7A.

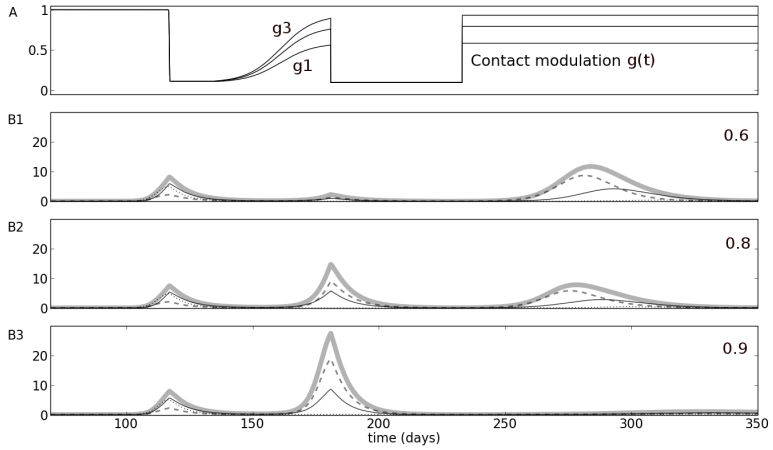

FIGURE 7. **Social distancing and school closures can create multiple outbreaks.** **A.** The different graphs show different modulations of the infection rate after behavioral changes occurred. **B1-B3.** Different time courses for the percentage of A-H1N1pdm cases. Panels B1, B2, and B3 correspond, respectively, to the curves g1-g3. The thick curves are the sum of all infected individuals. The strongly and weakly connected populations are shown in solid and dashed black lines, respectively. The values of the mean infection rate after behavioral changes have occurred noted in the right upper corner of each plot and correspond to the curves g1-g3 shown in panel **A**. Other parameters as in previous figures. The slope of the modulation function $g(t)$ after the relaxation of social distancing measures was 0.3. Other parameters: t_0=78 for Oaxaca and Veracruz as starting States.

As illustrated in Fig. 7B1-B3, the government policies implemented at the end of April do explain the decrease of the epidemic outbreak observed in the data for the first wave. Further, the second "wave" can be generated by several combinations of the slope and inflection time of the sigmoid used to resume of activity in May (after day 120). Furthermore, our simulations suggest that the second "wave" is the result of a rebound in the epidemic in which the susceptibles from the weakly connected States played a significant role. Our simulations suggest that second "wave" was also cut short by the reduction in contacts at the end of the school year. The start of classes for the fall in Mexico is typically around September 1. The third "wave" of the A-H1N1pdm in México starting around then. For this reason, the mechanism of suppression and recovery of the infection rates described in the last paragraphs was used again, in this case with sharp slopes representing the sudden changes in transmission that may occur during closure and reopening of schools. Taken together, these results suggest that the implementation of measures that decrease the contact rates in combination with the school calendar, as it was the case in México, can have a significant mitigating effect on the spread of the influenza.

The patterns shown by the strongly and weakly connected States in the different scenarios shown in Fig. 7B1-B3 also reflect nontrivial aspects of the epidemic. For instance, if the infection rate recovers to a small proportion of what it was originally (Fig. 7A, line labeled "g1", $g(t) \approx 0.5$, $t > 300$), infections would occur at a very

low rate after the government intervention. In this case, the model predicts that there would be only two large "waves" during the year with one outbreak of small amplitude during the summer, and a third "wave" occurring after a long delay (Fig. 7B1, thick gray line). In cases like these, the strongly connected populations would experience the bulk of the epidemic first (black, solid lines), followed by the weakly connected populations during the second "wave" (black, dashed lines).

As the recovery in the infection rate increases after the social distancing is relaxed, a second "wave" starts to emerge during the summer (Fig. 7B2), followed by a third wave that still occurs in the fall/winter ($0.3 < g(t) < 0.8$, $t > 300$). The contribution from the weakly connected States to the second "wave" is always more prominent than the contribution from the strongly connected States. Both strongly and weakly connected States contribute during the third "wave" of the fall/winter. However, the third "wave" starts first in the weakly connected States, followed by growth in the strongly connected States. If the final infection rate is large enough, the third "wave" starts at the strongly connected States (not shown). This occurs in part because during the second "wave" the weakly connected States are affected the most. That is, the (still large) susceptible population in the weak states is the driver for the second "wave". If the infection rate recovers almost fully (Fig. 7B2, $g(t) \approx 0.9$, $t > 300$), the second "wave" increases in size until the third "wave" does not occur anymore. Not surprisingly, if there are enough susceptibles after a decrease in contact that caused a decay in the epidemic curve, and there are no further interventions (e.g. vaccination), there will be a rebound "wave". The size depends on the size of the first outbreak.

The number of secondary outbreaks is highly dependent on the size of the first "wave", and the timing and impact of subsequent interventions. In particular, the size of secondary and later "waves" depends on the similarity between infection rates before and after each decrease in the incidence curves. In the context of the above simulations, if the behavioral changes just mentioned result in a reduction of the infection rate of approximately 35% or more, then the rebound "wave" can take several months to occur (Fig. 7B1). In contrast, if the reduction is less than 35% a significant rebound "wave" can take as little as 2 months to occur (Fig. 7B2). If the decrease in infection rates is about 10% or less the pool of susceptibles is almost completely depleted during the second (rebound) "wave", thus eliminating the possibility of a third "wave" (*e.g.* Fig. 7B3).

3.3. **Time course of epidemic by State.** We now describe simulations of the dynamics of the epidemic by State using parameters that resulted in three "waves" with a qualitatively similar time course to that shown in the data (Figs. 2 and 7B2). For instance, the second "wave" is milder and wider that the first one, and starts shortly before the summer. Also, the third "wave" is the strongest and occurs during the fall. An example of the temporal profile of the epidemic by State is shown in Fig. 8.

Local transportation patterns and changes in contacts during the epidemic as determined by social distancing measures and school closures are sufficient to generate specific aspects displayed by the data, including the delays between outbreaks in different populations (compare to Fig. 3). Importantly, these factors do not generate the patterns observed in the data when only transportation or behavior-dependent contact rates are considered in isolation. Fig. 8 clearly illustrates that the "waves" result from nonuniform aggregation of cases originated in the different Mexican States at different times during the year. Importantly, the change in the

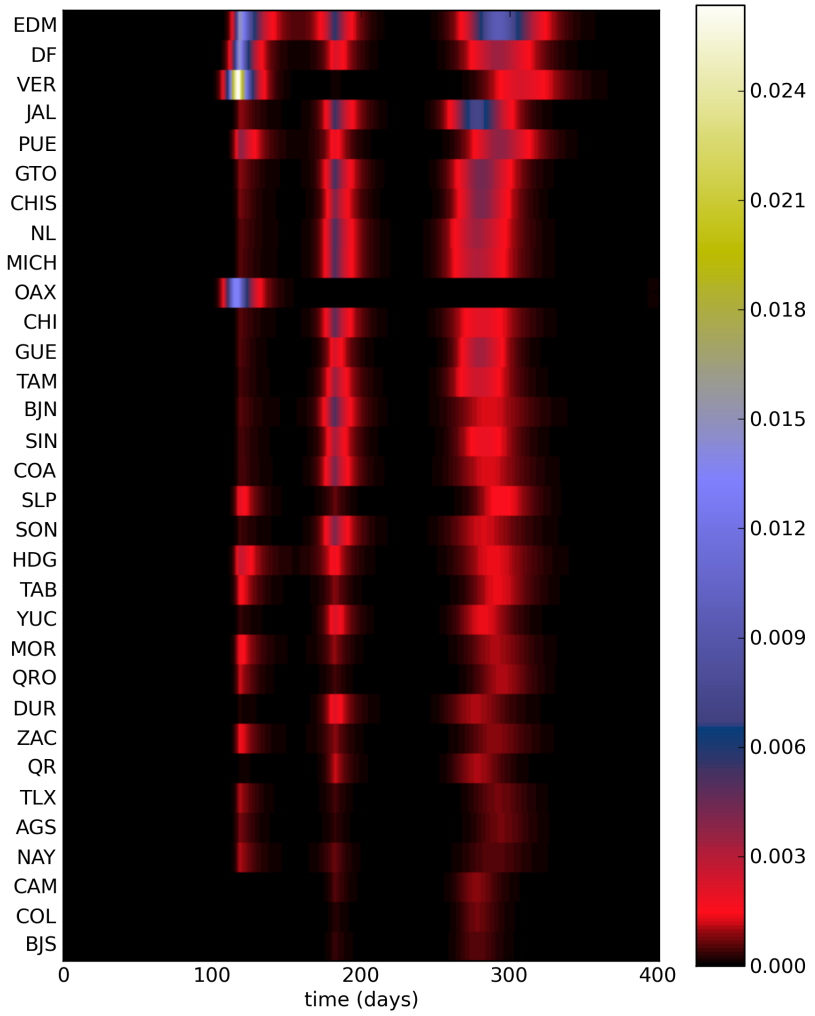

FIGURE 8. **Percentage of cases by State assuming the first cases were in Oaxaca and Veracruz.** The States have been ordered with respect to their population size.

transportation patterns during the summer break underlies the contribution of the pool of susceptibles in the weakly connected states to the second outbreak. In a similar way, the change in the transportation pattern prior to the return to classes in the fall favors the contribution of the susceptibles in the strongly connected populations to the third outbreak. It is during this third outbreak that most States experience an outbreak without interruptions. Importantly, these simulations also

highlight the possible risk of a more prominent rebound "wave" of influenza after social-distancing or school closure interventions if no further vaccination or other protective measures are implemented.

In the next section, the vaccination stockpile, ν, is assumed to be nonzero and the arrival date of the vaccines is systematically varied to study the effects of introducing vaccination at different points in time during the epidemic (Sec. 3.4). The idea is that in the event that a very contagious virus emerges, interventions as the one made by the Mexican government could help avoiding saturating the demand for resources destined to help the population when the initial outbreak and the next school closure are distant in time (at least 4 weeks). Further, a mitigation strategy to further constrain the spread of influenza through vaccination during the school break is conceivable by taking into account the dynamics shown in Figs. 7 and 8.

3.4. **Role of vaccination.** The simulations in Fig. 7 suggest that social distancing and school closures had a delaying effect on the transmission of the 2009 pandemic influenza virus, thus creating a window of opportunity to implement preventive measures such as vaccination. Therefore, we decided to examine the role that vaccination could have had in mitigating the last "intervention-free" outbreak.

Since it was clear from the beginning of the pandemic that supplies would be short for most of the countries in the world, we conducted simulations using the system (1)-(14) and assuming a limited number of vaccines are available. In this respect, the Mexican government announced that they would have a stockpile of nearly 30 million vaccines [66]. However, only a small fraction of the planned stockpile became available in November of 2009 (*ca.* 3% of 30 million). By mid January, only approximately 1.5 million had been distributed among the population [66].

To carry out the simulations, vaccination was introduced at different dates after the social distancing measures and school closures implemented by the Mexican government in April were suspended. The parameters for the simulations were the same as in Fig. 7B2 and Fig. 8 with a stockpile of 30 million vaccines and a maximum of 100,000 vaccines administered per day. For the simulations shown in Fig. 9, vaccinations were distributed throughout the different States in México according to their population size. That is, vaccination was not assumed to be proportional to the populations that received the vaccines as typically assumed in previous models (*e.g.* [67]). Simulations were carried out assuming that every person, except those who had been confirmed as SOIV-AH1N1 cases, received the vaccine. Vaccines were assumed to be distributed among the population as soon as they arrived.

The effects starting vaccination on July 18, Sept 5, Oct 25, and Dec 15 are shown in Fig. 9. These simulations suggest that if vaccination started at least in September, the impact on the epidemic outbreak would have been minimal (compare panels A and D in Fig. 9). On the other hand, if vaccination is introduced before November, the effects on the incidence curves are more drastic and become noticeable on or before September 5, at the beginning of the fall scholar term. An estimate of the effect of introducing vaccination at different times was calculated by dividing the integrals of the incidence curves for each of the arrival times by the integral of the incidence curve when no vaccination was introduced (not shown). The maximum decrease obtained with the stock pile and maximum number of vaccines that produced Fig. 9A was approximately 15% for the simulations performed here.

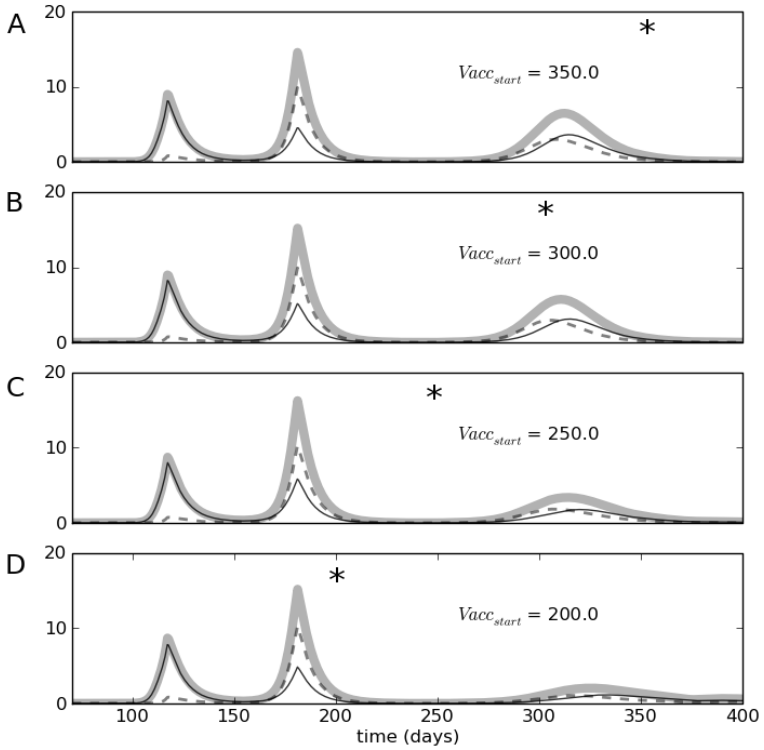

FIGURE 9. **Democratic vaccination for different arrival times.** Vaccination of a maximum of 100,000 individuals per day from a stockpile of 30 million. **A-D.** Time course of the epidemic assuming starting vaccination times at days 200, 250, 300, and 350, corresponding, respectively, to July 18, Sept 5, Oct 25, and Dec 15. Vertical axis, percentage of the population. Parameters as in Fig. 7.

In conclusion, the early arrival and application of vaccines could have had a noticeable but not too strong mitigating effect on the spread of the disease; even for stockpiles with as many vaccines as 30 percent the total population; a quantity that corresponds to the total of availability of vaccines originally announced by the Mexican government (see Morales et al., this volume). Further, our simulations indicate that the administration of the vaccines would have resulted in a significant waste after November since no visible effects on the size or time course of the epidemic curve could be observed in this case.

4. **Discussion.** The simulations presented here explain the existence of multiple "waves" in the data in terms of the combined effects of transportation patterns and behavioral changes. The behavioral changes are captured by considering the reductions in contact from social distancing measures implemented by the Mexican government, motivated by fear, or due to the school calendar. As expected, local transportation without a decrease the infection rates (social distancing) results in

single epidemic outbreaks; recall that the pattern of traffic is described by a star-shaped graph with two sets of populations contributing differently to the daily flow through the "center" node. The macroscopic patterns displayed by the regional and whole-country data may thus be a consequence of the differences in flow between the strongly and weakly connected states, and the drops in contact rates. From a macroscopic (whole-country) perspective, the model shows three "waves" when transportation and modulation of contact rates are combined (Fig. 7). However, when examined in detail, the "waves" result from the aggregation cases occurring non-uniformly with respect to location and time (Fig. 8). In addition, the multiple "waves" do not occur because of differences in the recovery time or susceptibility to infection due to geographical factors. These results provide strong support to the hypothesis that a combined effect of local transportation, social distancing, and school closures can produce multiple macroscopic (whole-country) "waves" for the same epidemic; as observed in México during 2009 (Fig. 2).

4.1. **Effects of behavioral modulation and intervention.** Our simulations unravel different possible scenarios in which influenza epidemics can occur for qualitatively similar time dependent changes in the infection rate (Fig. 7). Remarkably, the two U-shaped modulations in the infection rate used here did not always result in three large "waves". The "waves" in the cases considered here occur because the implementation of social distancing and school closure measures pause, but not stop, the spread of the disease. The novel A-H1N1pdm considered here is non-seasonal, so there are, a priori, no reasons to believe that the epidemic was mitigated by changes in temperature or weather at large. Our simulations show that the number of rebound "waves" depends on the number and steepness of U-shaped modulations in the infection rates but also on the final value of the contact-modulating function g. As a rule of thumb, a significant rebound in an epidemic outbreak can be observed after an intervention if, aside from the timing the intervention before the epidemic peak, contact between individuals is decreased and then allowed to increased to similar, if not smaller value relative to the original infection rate. This result highlights the importance of quantifying behavioral changes and the speed at which these changes occur during an epidemic outbreak [15]. Therefore, it would be beneficial for future epidemics to obtain data that helps estimate the dynamics of contact.

The social distancing measures implemented in Mexico were very strict, much stricter than would have been imposed in other countries, and the behavioral changes (hand washing, use of masks in cold days or crowded places, television and newspaper adds, jokes, etc) were still present during the summer of 2010 (MAHV personal observations). To the best of our knowledge, we interpret the first local maximum in the simulated epidemics as the result of reduced contact. We believe that the fall "wave" was actually reached in what we could think of as an outbreak free of intervention. The epidemic does not hit all the States during the first two "waves", but both weak and strongly connected States are affected during the third wave. This pattern is consistent with the data globally and locally (by State), but it is worth to remark that it is highly dependent on the behavioral modulation captured included in the infection rate. For instance, there would have been no third wave during the year if the behavioral changes in the population were short-lasting (g with a final value close to one and a fast positive slope after a decrease).

Government intervention during the initial stages of an epidemic outbreak can help to mitigate the spread of the infection. Governments can use this strategy to

initially mitigate the spread of influenza while resources become available. The price to pay for the initial mitigation may be an increased likelihood of a second, or even a third more prominent outbreak. An disturbing possibility is that if the necessary resources are not available when the full outbreak occurs, the consequences can be significant depending on the severity of the disease. In addition to the possible financial implications of a sudden reduction in the contact rates via the implementation of social distancing policies, an additional burden on the health care system could result from untimely interventions or interventions not followed by appropriate mitigation strategies. Therefore, mild virulence of the 2009 pandemic should be regarded as a luck factor that may not be present in future pandemics.

4.2. **Global dynamics emerged from local interactions.** The separation of States into strongly and weakly connected based on the initial report of the epidemic was partially consistent with historical evidence about a corridor of epidemic transmission [1]. Remarkably, assuming this initial division in the contribution to the flow through the central node in our model (DF) also resulted in local dynamical patterns of spread during the year that are consistent with the data separated by State (Fig. 7 and 8). Note that those States affected during the initial outbreak "wave" that were not in "the" influenza corridor belong to a subset of populations in México that have close commercial, touristic, and other interactions with México City. For instance, the State of Veracruz is the largest contributor of import/export goods to México and does not belong to States in "the" corridor. The simulated epidemics in those States are in reasonable agreement with the existing data, suggesting that the classification of States into weak and strong is an important factor in addition to the centralized traffic assumed in the transportation rates.

In Mexico, the social distancing measures were broad enough to affect the whole population. If the age profile of the traveling population was similar to the age profile of the population as a whole, the effect of age on travel would probably be of little importance. With less stringent distancing measures, school closures could have an effect, as the part of the population most involved in disease transmission is formed by students, and thus might have a larger effect than a homogeneous mixing model would indicate. Therefore, the question of whether school closures translated into a real decrease in contacts, as was probably the case in Mexico, or whether they translate into more time at day care centers or the mall, as might have been the effect in the US or Canada could be asked. In fact, it could be the case that, in addition to the changes in transportation, there was an increase in contact during the summer breaks. However, based on the model, such an increase would have happened mostly in the weakly connected States. In addition, the model was built assuming that people within each State would randomly mix. For these reasons, we conclude that the school closures did have an impact on the time course of the epidemic, but this impact was indirect, as the flow of transportation changed, and with it, the availability of susceptibles. Age structure was significant for H1N1, and its effects have been documented elsewhere in the case of single populations [57]. The effects of including age structure in the model presented here would be helpful to study questions related to how data might be aggregated over time in different parts of the population, and in particular, to tackle questions related to the direct or indirect role played by the school closure on the transmission dynamics.

4.3. **Timing the administration of a limited vaccine stockpile.** The simulations presented in Figs. 7 and 8 suggest that the school closures due to the calendar

can be used as reference time points to implement prevention strategies in anticipation of secondary epidemic outbreak. For instance, depending on the initial rate of change of the incidence in the outbreak, if the starting point is too far from the date of the next school break, it might be worth having a short lasting intervention like that implemented by the Mexican authorities. Such interventions might be costly from a financial perspective, but may prevent a challenge to the health care system that could be catastrophic. Importantly, as suggested by our simulations, such interventions will also cause rebound "waves". As a consequence, the interventions aimed to decrease contacts among the population should be thought of as a delay mechanism that should be followed by prevention strategies such as vaccination; delaying the spread also prevents people from acquiring immunity. The timing of the prevention strategies should be in sync with the times of the major school closures (summer, winter, and possibly spring breaks) and could be improved if coordinated with ongoing surveillance [21].

Our simulations corroborate in a quantitative way a prediction rooted in common sense: if the available vaccines are given to the population before the (third) epidemic "wave", the number of infected people will decrease dramatically, and by extension, less vaccines will be wasted. Our model can be very useful in the sense that possible scenarios can be planned if data is used together with the model to produce short-term predictions. For instance, our simulations suggest that the best time to vaccinate people in the case of México would have been during the summer. As a general rule of thumb, these results can be generalized as: "vaccination campaigns are more effective during school breaks". The reason, as suggested by our simulations and by existing data [53], is that the school breaks can be assumed to slow down epidemics of influenza (and similar viral diseases); on the flip side, the return to classes accelerates the spread of influenza. In fact, past studies have suggested that mass immunization of school children before vacation breaks would be an appropriate strategy for reducing the spread of influenza within communities [33, 35, 73, 72]. There are several reasons for targeting this group. First, school children are an easy group to reach and offer an excellent opportunity for mass immunization. School-based immunization programs or health fairs would preclude the need for a visit to a physician's office to receive the vaccine. Furthermore, children and schools are the major pathways that spread influenza to families and neighborhoods.

Importantly, with the current infrastructure to make vaccines, the vaccination strategy suggested here can only be conceived assuming a morbidity of the novel virus comparable to that of seasonal influenza. This strategy can be combined with ongoing surveillance [21] and generalized for its utilization in Latin America and other places where local transportation is similar to México. It is important to note here that the vaccine was not available in time to have much effect for the A-H1N1pdm epidemic, even with measures that postponed later waves. This will continue to be an important general feature of pandemics, unless ways to develop vaccines faster are found.

4.4. **Fitting procedure, emergent properties, and modeling vaccination.** The parameter ranges used in the simulations were obtained by fitting the rate of change in simulations to the data. Since the confirmed cases present in the data are just a proportion of the actual cases, the fitting was done by first scaling the simulations and the data to have a common maximum and only the rate of change during the initial upstroke of the epidemic was considered. Errors resulting

from this estimation procedure could be carried into our simulations and possibly bias our interpretation of the results. Two factors are reassuring in this respect. First, the parameters obtained in the fitting process were not disproportionate or in disagreement with estimations of the contact probabilities made by other groups [39, 23, 15, 8]. Second, based only the fitting to the initial outbreak dynamics, we obtain qualitatively similar time courses for epidemics of the whole-country and also State by State.

México is a country with many different environments, which in principle could affect the predisposition of the population to different immunological insults [45, 46] (see also [3, 68]). In particular, the recent trend of urbanization and aging of the Mexican population could be increasing the vulnerability to acute infectious respiratory diseases [1]. However, as noted before, the differences in the recovery time and infection rate by State were not enough to produce drastically different scenarios. In addition, the qualitative observations of the study presented in this article depend more on the modulation of the infection rates by behavioral changes than on the specific rates of infection or recovery. For these reasons, we are confident that our parameter estimation is within acceptable ranges, and that our results are not the consequence of making unrealistic assumptions.

We have also made some progress on the way vaccination is modeled. In this work we implemented a vaccination scheme in which not only there was a limit for the total number of vaccines available, but also, one that allowed saturation in the daily demand for vaccines. To do so, the number of people that can be vaccinated per day was calculated by first setting up a policy for the distribution of the stockpile by State, and with respect to that distribution policy, a maximum number of vaccines per State per day was calculated. The actual number of vaccines given per day was either the maximum per day, or less depending on how many people were present in each State, and each class. This scheme is very different in comparison to the typical assumption that a proportion of the population gets vaccinated at any point in time [67, 59, 60].

4.5. **Future directions and concerns raised by simulations.** The results obtained in this work could have been obtained with a simpler model only containing three classes, namely, unprotected, infected, and recovered. However, since the difference in computational cost between a simpler model and the one used here was hardly noticeable using the code and the laptop computers described in Methods, we decided to numerically solve Eqs. (1)-(14) which allow the extension into a model that enables the calculation of wasted vaccines and tackle other important issues.

For instance, there is a big problem with influenza data since many, perhaps most, cases are mild enough not to be recorded or noticed. Therefore, a significant fraction of disease transmission comes from people that are asymptomatic in this sense. The presence of a population of asymptomatic or unconfirmed cases has been documented to be non-negligible [4], and it is believed to be close to 80% or 90% of the infected people [30]. A more detailed analysis of aspects related to the unconfirmed population will appear elsewhere.

The second and the third "waves" observed during 2009 could be explained by drifts or shifts. Our model does not include the possibility of relapse, or that a different virus(es) indistinguishable with the current methods from the original one for which the recovered population would not be completely immune. Drifts of shifts could explain part of the second and the third "waves" observed during 2009. This is a direction that requires more exploration. A priori, based on an intuition

fixed by the simulations presented here and on the observations made about the different contributions to the number of confirmed cases by the different States, our interpretation is that the multiple "waves" resulted mostly from the combined dynamics of local transport and changes in contact rates. In other words, the magnitude of the incidence curves may change if different immunities are taken into account, but not the general trends related to the number of waves their timing with respect to the events that change the probability of contact between individuals. The proportional distribution scheme used here can be modified to accommodate rules or policies not necessarily based on the size of the local populations. For instance, the distribution of vaccines in this model can be defined so that it reflects different levels of geographical isolation, or other differences due to the political and economical constrains (say, due to the existence of "guerrilla" in some areas of the country, budget for cities as opposed to whole States, etc).

The effectiveness, supply, and capability of distribution of vaccines are aspects that have not been addressed in this work. Parameters that capture these features are hard to estimate for several reasons. There have been some problems with some of the stockpiles of the vaccination for the novel A-H1N1pdm virus. For instance, the week of November 16, the pharmaceutical company GlaxoSmithKline asked the Canadian authorities to recall a stockpile of about 176 thousand vaccines of the same kind that were supposed to arrive to México [48]. The reason for the recall in 6 of the 13 Canadian provinces and territories was suspected to cause more adverse reactions than normally expected (1 in 20 thousand). In consequence, there are many uncertainties about the supply of the vaccination and at this point it is hard to estimate the effectiveness of the vaccines against a new virus [26]. In addition, there have been several reports in the last months about antiviral resistance in some patients to oseltamivir (Tamiflu) [38, 54, 49]. Regardless of the issues discussed above, the uncertainty about the novel A-H1N1pdm outbreak seem to have been resolved in the sense that the epidemic did not have devastating effects in terms of mortality and the infection seems to be mild in comparison to other influenza types and subtypes [31, 61]. These studies and others aimed understand the transmission dynamics of highly virulent diseases like smallpox [18] are extremely important to assess the risk of treats like the deliberate release of biological agents among others.

4.6. **Final remarks.** Our results support the notion that the massive governmental intervention measures at the beginning of April did mitigate the spread of influenza but as a result exhaust the supply of susceptibles. In fact, the first two "waves" were interrupted by social distancing policies, the closing of schools in the summer, and altered by delays in transportation "effectiveness". The only intervention measures during that third "wave" came from the vaccination of a relatively small group of people that started at the end of November. In other words, México's transportation structure and the non-uniform flow of individuals over this network contributed significantly to the generation of three outbreaks; the third significantly larger (and over a longer time span) than the first two. The third outbreak of infection (Fig. 2) can therefore be thought of as the result of a fully operational network. The synergistic interactions between transport flow and modulation of the infection rate by social-distancing and school closures seem enough to cause the number of A-H1N1pdm cases to aggregate differently for the different States, thereby forming multiple peaks of different sizes (Fig. 2).

To summarize, social distancing and school closures have a delaying effect in the spread of the epidemic. However, the model suggests that an unprotected population is likely to suffer from a secondary or even a third harder epidemic outbreak in comparison to the initial wave if no further mitigation strategies are embraced. Governments can use a strategy based on this knowledge about the possible delays induced in an epidemic outbreak strategy to initially mitigate the spread of influenza while resources become available, but an alarming alternative is that if the resources are not available when the full outbreak occurs, the consequences can be significant depending on the severity of the disease. The A-H1N1pdm virus that caused the 2009 pandemic has been mild in terms of infection and mortality. As reports about transmission and recombination of different influenza viruses increase, and in view of the recent pandemic, which was caused by a novel form of the virus having portions of avian, porcine, and human A type influenza viruses, it may be worthwhile to destine more resources to increase the capacity of mass production of vaccines and treatment in preparation for a possibly more severe influenza epidemic in the future.

Acknowledgments. We thank anonymous reviewers for their suggestions. We also thank Gerardo Chowell-Puente for all of his comments, criticism, and for providing the template code to generate the map illustrations. We also thank José Vega for compiling the State data. A grateful acknowledgment for Julien Arino, Ping Yang, and Erin McKiernan for their challenging comments and recommendations.

REFERENCES

[1] R. Acuña-Soto, "Historical and Epidemiological Patterns of Influenza in México," In "Workshop: Mitigating the Spread of A/H1N1 Flu: Lessons Learned from Past Outbreaks," Arizona State University, 2009.

[2] R. Acuna-Soto, *Death records from historical archives: A valuable source of epidemiological information*, Mathematical and Statistical Estimation Approaches in Epidemiology, (2009), 189–194.

[3] F. S. Albright, P. Orlando, A. T. Pavia, G. G. Jackson and L. A. C. Albright, *Evidence for a heritable predisposition to death due to influenza*, The Journal of Infectious Diseases, **197** (2008), 18–24.

[4] L. K. Altman, "Many Swine Flu Cases Have no Fever," New York Times, 2009. URL http://www.nytimes.com/2009/05/13/health/13fever.html.

[5] V. Andreasen, J. Lin and S. A. Levin, *The dynamics of co-circulating influenza strains conferring partial cross-immunity*, Journal of Mathematical Biology, **35** (1997), 825–842. URL http://www.ams.org/mathscinet-getitem?mr=99a:92013.

[6] L. A. Angelova, *Long-term immunity to influenza A (H1N1) in humans*, In Annales de l'Institut Pasteur. Virologie, Elsevier, **133** (1982), 267–272.

[7] J. Arino and P. van den Driessche, *A multi-city epidemic model*, Mathematical Population Studies, **10** (2003), 175–193.

[8] J. Arino, F. Brauer, P. van den Driessche, J. Watmough and J. Wu, *A model for influenza with vaccination and antiviral treatment*, Journal of Theoretical Biology, **253** (2008), 118–130.

[9] O. V. Baroyan and L. A. Rvachev, *Deterministic models of epidemics for a territory with a transport network*, Cybernetics and Systems Analysis, **3** (1967), 55–61.

[10] S. Bertozzi, A. Kelso, M. Tashiro, V. Savy, J. Farrar, M. Osterholm, S. Jameel and C. P. Muller, *Pandemic flu: From the front lines. Interviewed by Declan Butler*, Nature, **461** (2009), 20.

[11] F. Brauer, *Compartmental models in epidemiology*, Mathematical Epidemiology, (2008), 19–79. URL http://www.ams.org/mathscinet-getitem?mr=2428372.

[12] F. Brauer and C. Castillo-Chavez, "Mathematical Models in Population Biology and Epidemiology," Springer Verlag, 2001.

[13] F. Brauer and C. Kribs-Zaleta, "An Introduction to Dynamical Systems for Biological Modeling" (series: chapman & hall/crc mathematical & computational biology), 2010.
[14] R. M. Bush, C. A. Bender, K. Subbarao, N. J. Cox and W. M. Fitch, *Predicting the evolution of human influenza A*, Science, **286** (1999), 1921.
[15] P. Caley, D. J. Philp and K. McCracken, *Quantifying social distancing arising from pandemic influenza*, Journal of The Royal Society Interface, **5** (2008), 631.
[16] C. Castillo-Chavez, H. W. Hethcote, V. Andreasen, S. A. Levin and W. Liu, "Cross-Immunity in the Dynamics of Homogeneous and Heterogeneous Populations," Mathematical Ecology, World Scientific, Singapore, page 303, 1988.
[17] C. Castillo-Chavez, H. W. Hethcote, V. Andreasen, S. A. Levin and W. M. Liu, *Epidemiological models with age structure, proportionate mixing, and cross-immunity*, Journal of Mathematical Biology, **27** (1989), 233–258, URL http://www.ams.org/mathscinet-getitem?mr=90g:92056.
[18] C. Castillo-Chavez, B. Song and J. Zhang, *An epidemic model with virtual mass transportation: the case of smallpox in a large city*, Bioterrorism: Mathematical Modeling Applications in Homeland Security, page 173, 2003. URL http://www.ams.org/mathscinet-getitem?mr=2036546.
[19] M. Chan, "Influenza A(H1N1)," Technical report, WHO, 2009. URL http://www.who.int/mediacentre/news/statements/2009/h1n1_20090429/en/index.html.
[20] G. Chowell, S. M. Bertozzi, M. A. Colchero, H. Lopez-Gatell, C. Alpuche-Aranda, M. Hernandez and M. A. Miller, *Severe respiratory disease concurrent with the circulation of H1N1 influenza*, The New England Journal of Medicine, **361** (2009), 674.
[21] G. Chowell, C. Viboud, X. Wang, S. M. Bertozzi and M. A. Miller, *Adaptive vaccination strategies to mitigate pandemic influenza: Mexico as a case study*, 2009.
[22] G. Chowell, C. Viboud, L. Simonsen, M. A. Miller and R. Acuna-Soto, *Mortality patterns associated with the 1918 influenza pandemic in Mexico: Evidence for a spring herald wave and lack of preexistingiImmunity in older populations*, The Journal of Infectious Diseases, 2010.
[23] V. Colizza, A. Barrat, M. Barthelemy, A. Valleron and A. Vespignani, *Modeling the worldwide spread of pandemic influenza: Baseline case and containment interventions*, PLoS Medicine, **4** (2007), 95.
[24] J. A. Córdova-Villalobos, *Lessons learned and preparing for the future: Influenza a/h1n1 in méxico*, Plenary 1, Encuentro Actualización Eninfluenza A (H1N1): "Lecciones Aprendidas y Preparándonos para el Futuro," Cancún, México, 2009.
[25] R. B. Couch and J. A. Kasel, *Immunity to influenza in man*, Annual Reviews in Microbiology, **37** (1983), 529–549.
[26] G. Del Giudice, K. J. Stittelaar, G. van Amerongen, J. Simon, A. D. M. E. Osterhaus, K. Stöhr and R. Rappuoli, *Seasonal influenza vaccine provides priming for A/H1N1 immunization*, Science Translational Medicine, **1** (2009), 12re1.
[27] Instituto Mexicano del Transporte, *North american transportation statistics database*, 2006–. URL http://nats.sct.gob.mx/nats/sys/index.jsp?i=3.
[28] M. Falco, *Cdc: Production of h1n1 flu lagging*, 2009. URL http://www.cnn.com/2009/HEALTH/10/16/h1n1.vaccine.delay/index.html#cnnSTCText.
[29] Z. Feng, W. Huang and C. Castillo-Chavez, *On the role of variable latent periods in mathematical models for tuberculosis*, Journal of Dynamics and Differential Equations, **13** (2001), 425–452.
[30] A. Flahault, X. De Lamballerie and T. Hanslik, *Symptomatic infections less frequent with H1N1pdm than with seasonal strains*, 2009.
[31] T. Garske, J. Legrand, C. A. Donnelly, H. Ward, S. Cauchemez, C. Fraser, N. M. Ferguson and A. C. Ghani, *Assessing the severity of the novel influenza A/H1N1 pandemic*, British Medical Journal, **339** (2009), b2840.
[32] Mexico City guide, "Transport," 2010. URL http://www.mexicocity-guide.com/transport.htm.
[33] M. Haber, I. R. A. M. Longini JR and M. E. Halloran, *Measures of the effects of vaccination in a randomly mixing population*, International Journal of Epidemiology, **20** (1991), 300.
[34] K. Hadeler and C. Castillo-Chavez, *A core group model for disease transmission*, Mathematical Biosciences, **128** (1995), 41–55.
[35] M. E. Halloran, M. Haber, I. M. Longini Jr and C. J. Struchiner, *Direct and indirect effects in vaccine efficacy and effectiveness*, American Journal of Epidemiology, **133** (1991), 323.

[36] W. Huang, K. L. Cooke and C. Castillo-Chavez, *Stability and bifurcation for a multiple-group model for the dynamics of HIV/AIDS transmission*, SIAM Journal on Applied Mathematics, 835–854, 1992.

[37] J. Hunter, D. Dale and M. Droettboom, "Matplotlib: A Python 2d Plotting Library," 2008–. URL http://matplotlib.sourceforge.net/.

[38] A. C. Hurt, J. Ernest, Y. M. Deng, P. Iannello, T. G. Besselaar, C. Birch, P. Buchy, M. Chittaganpitch, S. C. Chiu, D. Dwyer, et al., "Emergence and spread of oseltamivir-resistant A (H1N1) influenza viruses in Oceania, South East Asia and South Africa," Antiviral Research, 2009.

[39] E. S. Hurwitz, M. Haber, A. Chang, T. Shope, S. Teo, M. Ginsberg, N. Waecker and N. J. Cox, *Effectiveness of influenza vaccination of day care children in reducing influenza-related morbidity among household contacts*, The Journal of the American Medical Association, **284** (2000), 1677.

[40] J. M. Hyman and T. Laforce, *Modeling the spread of in fluecnza among cities*, Biomathematical Modeling Applications for Homeland Security, Philadephia: Society for Industrial and Applied Mathematics, 215–240, 2003. URL http://www.ams.org/mathscinet-getitem?mr=2036548.

[41] E. Jones, T. Oliphant, P. Peterson, et al., "SciPy: Open Source Scientific Tools for Python," 2001–. URL http://www.scipy.org/.

[42] W. O. Kermack and A. G. McKendrick, *Contributions to the mathematical theory of epidemics-I*, Proceedings of the Royal Society, **115A** (1927), 700–721 (Reprinted in Bulletin of Mathematical Biology, **53** (1991), 33–55).

[43] K. Khan, J. Arino, W. Hu, P. Raposo, J. Sears, F. Calderon, C. Heidebrecht, M. Macdonald, J. Liauw, A. Chan, et al., *Spread of a novel influenza A (H1N1) virus via global airline transportation*, The New England Journal of Medicine, **361** (2009), 212.

[44] C. D. Kozul, K. H. Ely, R. I. Enelow and J. W. Hamilton, *Low-dose arsenic compromises the immune response to influenza a infection in vivo*, Environ Health Perspect. PubMed, **117** (2009), 1441–1447.

[45] R. J. Kurukulaaratchy, S. Matthews and S. H. Arshad, *Does environment mediate earlier onset of the persistent childhood asthma phenotype?*, Pediatrics, **113** (2004), 345.

[46] P. R. S. Lagacé-Wiens, E. Rubinstein and A. Gumel, "Influenza Epidemiology: Past, Present, and Future," Critical Care Medicine, 2010.

[47] M. A. Lezana-Fernández, "A/h1n1 Epidemic in México: Lessons Learned," Talk at "Mitigating the Spread of A/H1N1 Flu: Lessons Learned from Past Outbreaks Workshop," Arizona State University, 2009.

[48] F. Libenson, "Llegaron al Edomex 66 mil Vacunas Contra AH1N1," 2009. http://elinformantemexico.com/index.php/noticias/llegaron-al-edomex-66-mil-v acunas-contra-ah1n1-franklin-libenson-violante.html.

[49] H. C. Lin, M. J. Chen, S. J. Chang, M. T. Liu, H. S. Wu, J. H. Chuang, J. H. Chou, H. S. Kuo and S. C. Chang, *Investigation of the first two cases of oseltamivir-resistant pandemic (H1N1) 2009 virus in Taiwan*, Taiwan Epidemiology Bulletin, (2009), 815–828.

[50] M. López-Cervantes, A. Venado, A. Moreno, R. L. Pacheco-Domínguez and G. Ortega-Pierres, *On the spread of the novel influenza A (H1N1) virus in Mexico*, The Journal of Infection in Developing Countries, **3** (2009), 327.

[51] Mexicocity.com.mx, "Taxi Cabs," 2010. URL http://www.mexicocity.com.mx/taxis2.html.

[52] M. A. Miller, C. Viboud, M. Balinska and L. Simonsen, *The signature features of influenza pandemics–implications for policy*, The New England Journal of Medicine, **360** (2009), 2595.

[53] A. S. Monto, *Interrupting the transmission of respiratory tract infections: Theory and practice*, Clinical Infectious Diseases, **28** (1999), 200–204.

[54] A. Moscona, *Global transmission of oseltamivir-resistant influenza*, The New England Journal of Medicine, 2009.

[55] M. R. Moser, T. R. Bender, H. S. Margolis, G. R. Noble, A. P. Kendal and D. G. Ritter, *An outbreak of influenza aboard a commercial airliner*, American Journal of Epidemiology, **110** (1979), 1.

[56] M. I. Nelson and E. C. Holmes, *The evolution of epidemic influenza*, Nature Reviews Genetics, **8** (2007), 196–205.

[57] H. Nishiura, C. Castillo-Chavez, M. Safan and G. Chowell, *Transmission potential of the new influenza A (H1N1) virus and its age-specificity in Japan*, Euro Surveill, **14** (2009), 19227.

[58] SSA Notimex, "Este Lunes Llegan las Vacunas Contra Influenza AH1N1," Notimex, 2009. URL http://www2.esmas.com/noticierostelevisa/mexico/nacional/116742/este-lunes-llegan-vacunas-contra-influenza-ah1n1.

[59] M. Nuno, G. Chowell and A. B. Gumel, *Assessing the role of basic control measures, antivirals and vaccine in curtailing pandemic influenza: Scenarios for the US, UK and the Netherlands*, Journal of the Royal Society Interface, **4** (2007), 505.

[60] M. Nuno, G. Chowell, X. Wang and C. Castillo-Chavez, *On the role of cross-immunity and vaccines on the survival of less fit flu-strains*, Theoretical Population Biology, **71** (2007), 20–29.

[61] A. Pedroza, J. G. Huerta, M. de la Luz Garcia, A. Rojas, I. López-Martínez, M. Penagos, C. Franco-Paredes, C. Deroche and C. Mascareñas, *The safety and immunogenicity of influenza vaccine in children with asthma in Mexico*, International Journal of Infectious Diseases, **13** (2009), 469–475.

[62] J. B. Plotkin, J. Dushoff and S. A. Levin, *Hemagglutinin sequence clusters and the antigenic evolution of influenza A virus*, Proceedings of the National Academy of Sciences, **99** (2002), 6263.

[63] L. A. Rvachev and I. M. Jr. Longini, *A mathematical model for the global spread of influenza*, Mathematical Biosciences, **75** (1985), 3–22. URL http://www.ams.org/mathscinet-getitem?mr=800965.

[64] A. N. Slepushkin, E. I. Bourtseva, A. L. Belyaev, L. N. Vlassova and E. L. Feodoritova, *Influenza morbidity and some peculiarities of antiinfluenza immunity and prevention during influenza pandemics*, In International Congress Series, Elsevier, **1263** (2004), 787–790.

[65] E. Spackman, D. E. Stallknecht, R. D. Slemons, K. Winker, D. L. Suarez, M. Scott and D. E. Swayne, *Phylogenetic analyses of type A influenza genes in natural reservoir species in North America reveals genetic variation*, Virus Research, **114** (2005), 89–100.

[66] SSA, "Situación Actual de la Epidemia [Current Epidemic Situation]," January 2010. URL http://portal.salud.gob.mx/contenidos/noticias/influenza/estadisticas.html.

[67] C. Sun and Y. H. Hsieh, *Global analysis of an SEIR model with varying population size and vaccination*, Applied Mathematical Modelling, 2009.

[68] R. A. Trammell and L. A. Toth, *Genetic susceptibility and resistance to influenza infection and disease in humans and mice*, Expert Review of Molecular Diagnostics, **8** (2008), 515–529.

[69] B. Valadez, "Aplicadas, Solo 10% de las Dosis Contra el A/H1N1," 2010. URL http://www.milenio.com/node/368812.

[70] C. Viboud, P. Y. Boélle, S. Cauchemez, A. Lavenu, A. J. Valleron, A. Flahault and F. Carrat, *Risk factors of influenza transmission in households*, In International Congress Series, Elsevier, **1263** (2004), 291–294.

[71] C. Viboud, O. N. Bjornstad, D. L. Smith, L. Simonsen, M. A. Miller and B. T. Grenfell, *Synchrony, waves, and spatial hierarchies in the spread of influenza*, Science, **312** (2006), 447.

[72] D. Weycker, J. Edelsberg, M. Elizabeth Halloran, I. M. Longini, et al., *Population-wide benefits of routine vaccination of children against influenza*, Vaccine, **23** (2005), 1284–1293.

[73] T. White, S. Lavoie and M. D. Nettleman, *Potential cost savings attributable to influenza vaccination of school-aged children*, Pediatrics, **103** (1999), e73.

[74] Wikipedia, "World Population 1800-2100," 2010–. URL http://en.wikipedia.org/wiki/File:World-Population-1800-2100.png.

Received June 1, 2010; Accepted September 21, 2010.

E-mail address: Marco.Herrera-Valdez@asu.edu
E-mail address: mcruzapo@asu.edu
E-mail address: ccchavez@asu.edu